Exp Fluids (2011) 50:613–620
DOI 10.1007/s00348-010-0964-3

RESEARCH ARTICLE

Three-dimensional particle tracking method using FPGA-based real-time image processing and four-view image splitter

Mark Kreizer · Alex Liberzon

Received: 31 March 2010 / Revised: 4 August 2010 / Accepted: 13 August 2010 / Published online: 26 August 2010

Abstract We present a cost-effective solution of the three-dimensional particle tracking velocimetry (3D-PTV) system based on the real-time image processing method (Kreizer et al. Exp Fluids 48:105–110, 2010) and a four-view image splitter. The image processing algorithm, based on the intensity threshold and intensity gradients estimated using the fixed-size Sobel kernel, is implemented on the field-programmable gate array integrated into the camera electronics. It enables extracting positions of tracked objects, such as tracers or large particles, in real time. The second major component of this system is a four-view split-screen device that provides four views of the observation volume from different angles. An open-source ray-tracing software package allows for a customized optical setup for the given experimental settings of working distances and camera parameters. The specific design enables tracking in larger observation volumes when compared to the designs published up to date. The present cost-effective solution is complemented with open-source particle tracking software that receives raw data acquired by the real-time image processing system and returns trajectories of the identified particles. The combination of these components simplifies the 3D-PTV technique by reducing the size and increasing recording speed and storage capabilities. The system is capable to track a multitude of particles at high speed and stream the data over the computer network. The system can provide a solution for the remotely controlled tracking experiments, such as in microgravity, underwater or in applications with harsh experimental conditions.

M. Kreizer · A. Liberzon (✉)
Turbulence Structure Laboratory,
School of Mechanical Engineering,
Tel Aviv University, Ramat Aviv 69978, Israel
e-mail: alexlib@eng.tau.ac.il

M. Kreizer · A. Liberzon
International Collaboration for Turbulence Research (ICTR),
Goettingen, Germany

1 Introduction

Lagrangian description of turbulent flows attracts increasing attention due to its simple conceptual basis and direct relation to the studies of transport, mixing and dispersion (Toschi and Bodenschatz 2009). Optical tracking of small particles, bubbles or droplets, is one of the major tools used to obtain Lagrangian trajectories for turbulence research Dracos (1996); Lüthi et al. (2005). With continuously increasing recording speed of imaging devices, the limitations have shifted to streaming and storage of the high-speed video data. High-speed digital cameras can record video at few gigabytes per second, but cannot transfer more than hundreds of megabytes per second to the storage device. A possible solution is a real-time compression, e.g. Chan et al. (2007) that reduces the data rate by a factor of 100–1000. For the tracking of sparse small objects, we proposed to decrease the data rate differently, implementing real-time image processing algorithm on the field-programmable gate array (FPGA) (Kreizer et al. 2010). The system can detect and localize a thousand particles in real time. The main advantage of the FPGA integrated in the camera electronics, rather than on an external device, is the strongly reduced data transfer rate. This enables operation of the remotely controlled camera using the existing network protocols and devices and significantly improves the mobility of particle tracking systems. In the present study, we extend the system for the three-dimensional particle tracking at high speed, instrumenting a real-time

image processing camera tracking with a four-view split-screen optical device. Similar optical designs have been used in a single camera stereoscopic particle image velocimetry (PIV) (e.g. Arroyo and Greated 1991; e.g. Bardet et al. 2010), and particle tracking experiments (e.g. Tsorng et al. 2006; Hoyer et al. 2005; Guala et al. 2008) used a multi-mirror optical setup to obtain three-dimensional particle tracking. The present optical setup has slightly different design, aimed at tracking of particles in larger observation volumes, when compared to the splitter design of Hoyer et al. (2005). The presented remotely controlled single-camera 3D particle tracking system can be useful for the large-scale tracking experiments (Lobutova et al. 2009), microgravity experiments (Dupont et al. 1999), or underwater applications (Nimmo Smith 2008). The system enables high-speed image recording rates and does not require synchronization of multiple cameras. However, due to a smaller number of pixels per view, one has to compromise the lower particle seeding density, when compared to the multi-camera systems.

The paper is organized as follows. Sect. 2 describes in detail the optical design and the three-dimensional particle tracking experiment setup. We report on the quality tests and preliminary results in Sect. 3 and summarize it in Sect. 4.

2 Experimental method

2.1 Experimental setup

We use a lid-driven cavity flow facility, described in detail in Kreizer et al. (2010). The flow facility and the experimental and optical setups are shown schematically in Fig. 1. The flow in the cavity (1) is driven by a belt (2) that slides above the glass tank. The speed of the belt is controlled by the computer-managed AC motor. We use a high-speed digital CMOS camera of 1280 × 1024 pixels @ 500 frames-per-second with a pixel size of 12 μm (MC1324, Mikrotron GmbH, Germany), with an integrated FPGA. The camera can transfer raw images or processed data through an Ethernet cable to a host PC, using GigE protocol. The processed data contains the positions of the center-of-mass and intensity of the particles in image coordinates, obtained from the x and y pixel coordinates of the left/right/top/bottom edges, the sum of the intensity values in horizontal and vertical direction and total intensity of the original particle. Details of the image processing algorithm were presented in Kreizer et al. (2010), along with the two-dimensional tracking and PIV results in the lid-driven cavity flow.

The main purpose of the new development is to develop a 3D tracking system that will complement the existing high-speed 3D-PTV system for the two-phase flow experiment similar to Guala et al. (2008). In the two-phase flow experiment, the existing multi-camera system could track densely seeded flow tracers, whereas the present system will track the large solid particles. Therefore, as a test case, we present particle tracking of relatively large, neutrally buoyant polystyrene particles [$d_p \approx 700$ μm, $\rho_p = 1.03$ g cm^{-3}, $\mathrm{S_t} \sim O(0.1)$] . This experiment is better suitable for the single-camera system which, due to the reduced number of pixels per view, requires lower volume fraction of the seeding material.

2.2 Optical setup

Our focus is on the extension that enables the three-dimensional Lagrangian particle tracking. We designed a four-view split-screen optical device (denoted as (3) in Fig. 1a and shown in orthogonal views in Fig. 1b), hereinafter called "image splitter", and an array of back-side mirrors such that the camera records four views of the cavity, as shown in the top view of Fig. 1b.

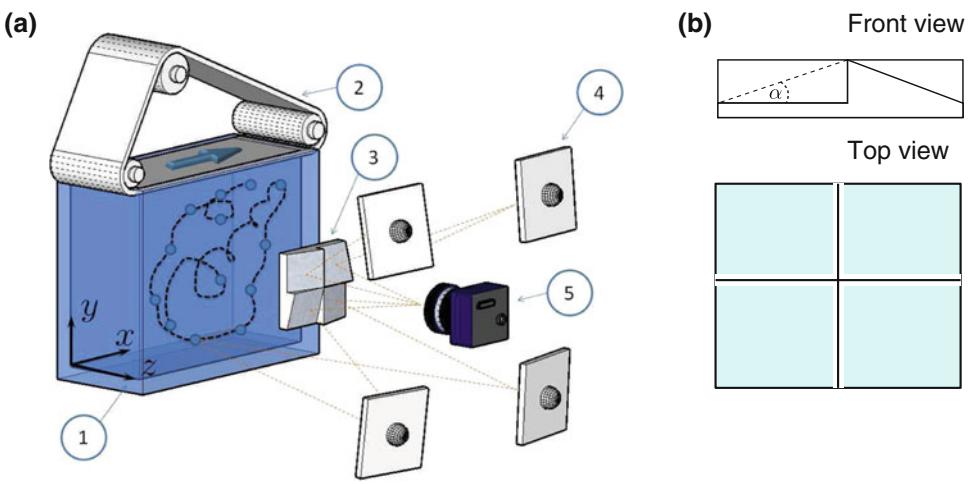

Fig. 1 **a** Schematic view of the lid-driven flow facility and the experimental setup. (1) cavity, (2) driving belt system, (3) four-view image splitter , (4) back-side mirrors, (5) the camera. **b** Orthogonal views of the four-view image splitter. *Shaded region* denote the useful imaging area

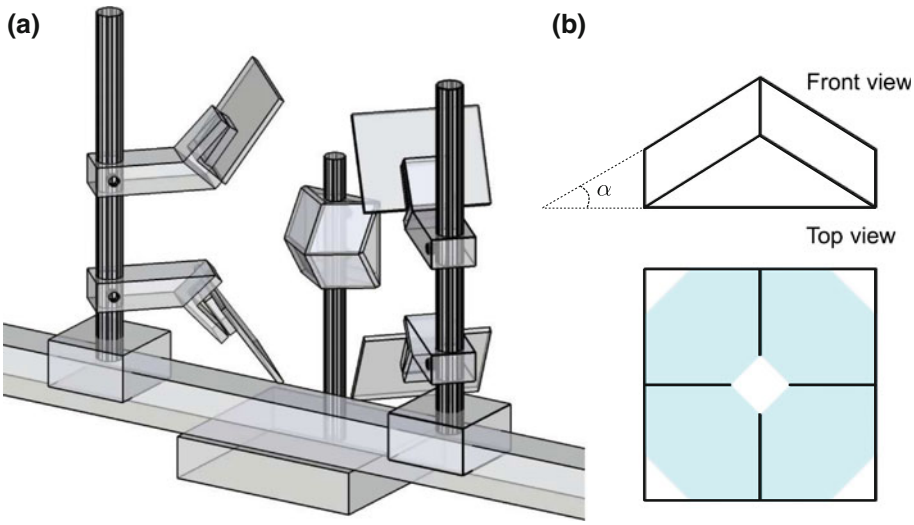

Fig. 2 **a** Schematic view of the optical setup (ETH Zurich design) of the image splitter design according to Hoyer et al. (2005). **b** Orthogonal views of the splitter. The *shaded region* is the useful image plane area. The central part and the corners are not covered at large front angles

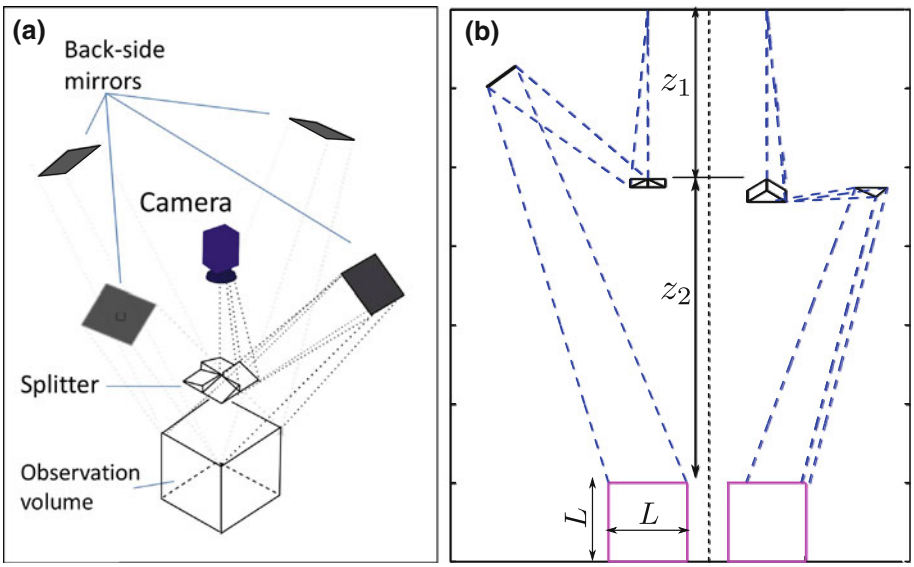

Fig. 3 Output of the open-source Matlab® toolbox showing the location and orientation of the optical setup. **a** Isometric view of our original design. **b** Comparative analysis of the ETH Zurich design (*right side*) and the original design (*left side*). The main parameters are distance between the view splitter, z_1, between the splitter and the observation volume, z_2, the length of the imaging path (*dashed lines*), and the position of the back-side mirrors

Four-mirror optical designs that enable only stereoscopic recording of two views mentioned previously (e.g. Arroyo and Greated 1991, among others; e.g. Tsorng et al. 2008, among others; e.g. Bardet et al. 2010, among others) are not directly applicable to the four-view design. The only known design that was implemented for the three-dimensional measurements is due to Hoyer et al. (2005); Guala et al. (2008), schematically shown in Fig. 2.

Prior to the new optical design of the image splitter, we attempted to use the design of Hoyer et al. (2005). Due to its relative large angle α, the back-side mirrors have to be positioned in the same plane with the splitter (see Fig. 3b). This leads to relatively large angles at which the four views are obtained and significantly reduces the observation volume that is an intersection of the four views. In addition, in some cases, the large angle of intersection and the close position of the back-side mirrors lead to undesired optical overlaps of the various views, decreasing the useful image plane area (shown in shaded regions in Fig. 2b). Therefore, we designed another image splitter, shown above in Fig. 1b. The new setup contains four symmetrical mirrors inclined at $\alpha = 16°$. This design has slightly better use of the image plane when compared to the design of Hoyer et al. (2005) (and 20% better, when compared to a simple four-sided pyramid). A smaller angle allows us to position the back-side mirrors at any plane between the splitter and the image plane. The new design is shown in projection in Fig. 3a, and the two designs are compared in Fig. 3b. Effectively, if the camera is located at some distance $(z_1 + z_2)$ from the cavity of 80 × 80 × 80 mm, the new design enables a smaller angle of intersection and a larger field of view. In the course of system development, an in-house open-source Matlab® toolbox was developed (available from the Turbulence Structure Laboratory website: http://www.eng.tau.ac.il/efdl).

Table 1 Parameters of the preliminary tests of the real-time image processing algorithm, shown in Fig. 4

#	Distance to the target (mm)	Number of dots in the field of view	Dot size (pixel)	True detections	False detections	Detection rate (%)
1	1,200	980	2 ± 1	967	3	98.3
2	800	354	5 ± 2	352	0	99.4
3	600	210	15 ± 3	207	1	98.1
4	300	60	40 ± 5	59	1	96.6

The inputs are geometrical and optical parameters: size of the imaging sensor, working distance, size of the observation volume and the distances between the imaging plane, the four-view splitter and the observation volume, denoted as z_1, z_2 in Fig. 3b. The software performs ray tracing analysis of the imaging paths between the camera and the measurement volume in order to estimate the positions and the angles of the back-side mirrors. It is possible to optimize the design varying the angle α of the front-side mirrors, the size of the splitter, position and orientation of the back-side mirrors. In appreciation of the comments of our anonymous reviewers, we also added the design of Hoyer et al. (2005) to the list of possible designs, as is shown in Fig. 3.

3 Results

3.1 Image processing test

The real-time image processing algorithm was tested for the two-dimensional particle tracking velocimetry in Kreizer et al. (2010). In two-dimensional experiments, all the particles are from the same focal plane and therefore approximately of the same size. There is no variation of the particle image as a function of the depth of view. The situation is different in the three-dimensional experiment—the size of the particles and their intensity vary significantly as they move in and out of the focal plane (in z direction). The image of the particle captured by the camera depends on many parameters, such as particle physical size, its optical properties (reflection/diffraction), distance between the camera and the particle, lenses, illumination conditions, sensor sensitivity, among others. Therefore, our first task is to test that an image processing algorithm can detect bright objects on a dark background under various conditions.

In this test, we used a planar calibration target that is typically used in PIV experiments: a thick plate made of stainless steel with an anti-reflective (black) background and white dots distanced 5×5 mm with a sub-micron precision. We tested the algorithm performance on images of the target taken at four different working distances between the camera and the calibration body (without the image splitter), reported in Table 1. At each distance, two sets of images were produced by the camera—a raw (unprocessed) image and a processed image saved in a binary format. We re-create an image out of the binary format files in order to visualize the data recorded and test the algorithm performance. The results are shown in Fig. 4 for the four distances, 1.2, 0.8, 0.6 and 0.3 m. Detection rate was estimated as follows:

$$\text{Detection rate} = \frac{\text{True detections} - \text{false detections}}{\text{Total number of dots}} \quad (1)$$

The results of the four tests are summarized in the following Table 1.

The preliminary test verified that the image processing algorithm could detect particles where the image size varied between 2 and 25 pixels with sufficiently high detection rate.

An additional performance test was performed in order to identify the smallest possible object size that can be detected by the real-time process under realistic illumination conditions (not shown here for the sake of brevity). Calibration target was illuminated by a collimated beam of approximately 0.05 m in diameter by the Nd:YLF laser (22.5 mJ/pulse, Quantronix Darwin Duo). The real-time image processing algorithm successfully detected dots at a large distance, showing its ability to track small flow tracers (of the order of 10 μm in diameter) in the given flow facility.

3.2 Calibration test

Calibration is the first procedure in three-dimensional particle tracking, during which the images of 3D objects are captured and processed in order to obtain the camera external and internal parameters Dracos (1996). It is important to test the calibration process using the optical setup. In this test, we used three-dimensional, multi-plane calibration target, shown in Fig. 5a. This target has dots at two planes (the difference is 1 mm), and it can be shifted back and forth using parallel slots manufactured with high accuracy. An example of the image of the four views, divided by the image splitter and recorded in the normal mode, is presented in Fig. 5b. This is a screenshot of the

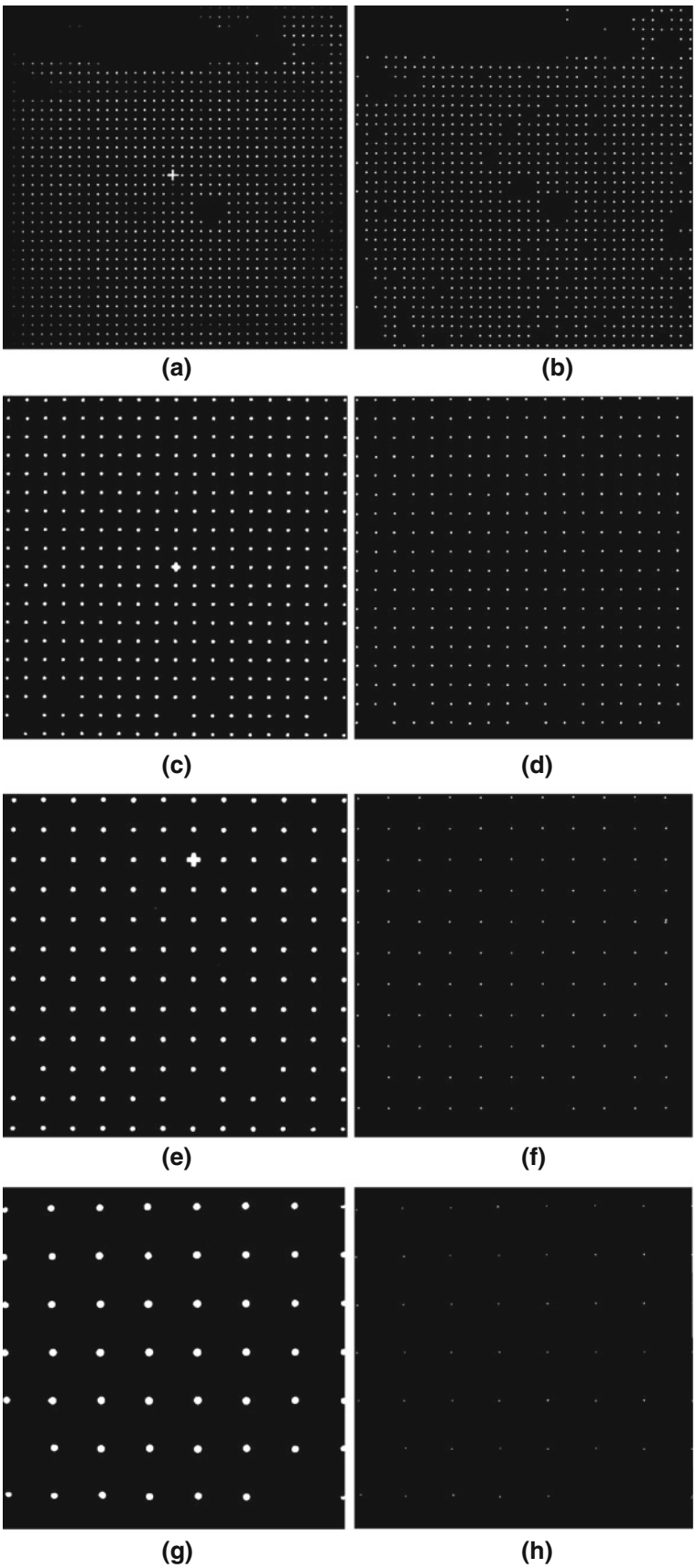

Fig. 4 Example images of the calibration body at different working distances: 1,200, 800, 600 and 300 mm for (a,b), (c,d), (e,f) and (g,h), respectively. *Left panel* is the unprocessed images (a,c,e,g) and right panel is the reconstructed image based on the raw data produced by the real-time algorithm (b,d,f,h). The quantitative summary of the results is given in Table 1 in the respective order of the test sets. The real data output is a 20-byte per-dot binary file, which is not formatted or transferred as an image

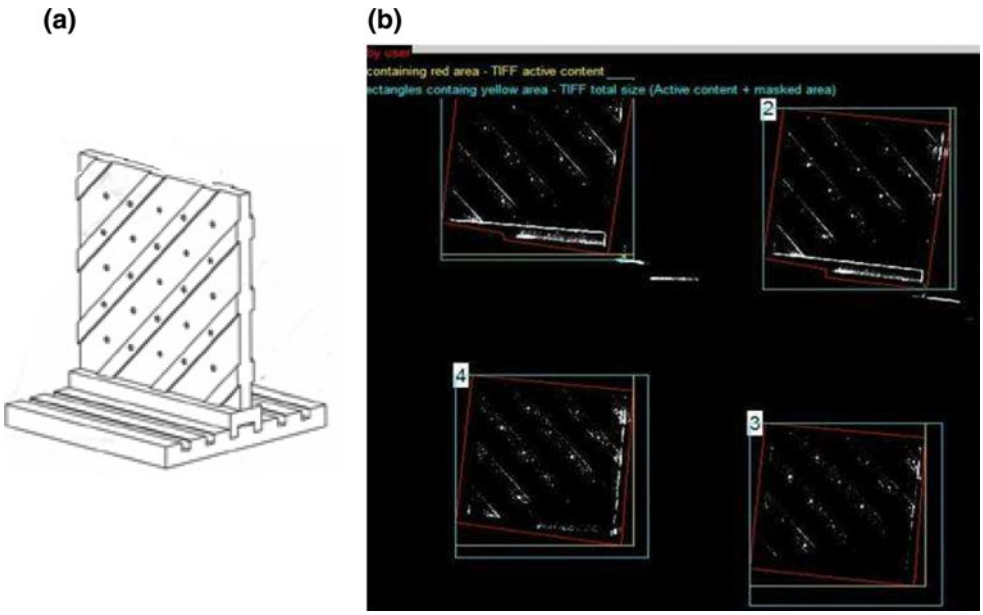

Fig. 5 **a** Multi-plane calibration target, used in the 3D-PTV experiment. **b** Snapshot of the four views of the multi-plane calibration target recorded via the unprocessed mode of the camera

Matlab® toolbox that allows for selecting four regions-of-interest in the image, which will be later used in the tracking and post-processing routines. The calibration was performed using the raw image, shown in Fig. 5b, applying standard 3D-PTV photogrammetric calibration procedure described by Lüthi et al. (2005); Guala et al. (2008). The output is four imaging models (one for each view) that are used later by the 3D-PTV software in order to convert the particle positions into the respective particle location in space (x, y, z). The imaging models could be improved during the experiment, using the particle positions.

3.3 Tracking test

The major results of the particle tracking velocimetry experiment are Lagrangian trajectories defined as locations of particles in time and space, $\boldsymbol{X}(t)$ (see for example, Fig. 6a). It is noteworthy that particles used in this experiment are neutrally buoyant but finite-sized and therefore, despite their low Stokes number of the order of 0.1, do not necessarily follow the turbulent flow.

We used the 3D-PTV algorithm reviewed in Dracos (1996) and improved by Lüthi et al. (2005). Traceability of the finite-sized particles with a relatively low seeding density is approximately 90%, i.e. 9 out of 10 identified particles were tracked. Trajectories, each at least 200 time steps long, are shown in Fig. 6b. We note that the particles were distributed in the cavity, unlike the results of Tsorng et al. (2006); Tsorng et al. (2008) who reported particles moving primarily in the x–y plane far from the walls. We can attribute this discrepancy to the three-dimensional optical setup, smaller particles and longer recording times when compared to Tsorng et al. (2006).

3.4 Velocity and acceleration tests

Probability density functions (PDF) of the velocity vector components, estimated as Lagrangian derivatives of the particle positions in time, $\boldsymbol{V}(t) = D\boldsymbol{X}(t)/D(t)$, are shown in Fig. 7a. Estimating velocity, one has to take into account the inherent errors of particle tracking velocimetry, analyzed in detail by Lüthi et al. (2005). These are mainly due to the calibration inaccuracy, estimated in our experiment of the order of 10 μm, error in subpixel accuracy of the particle center-of-mass detection (1/3 of the particle image size, in our case 0.7–1.1 pixel) and interpolation involved in tracking, which is effectively a low-pass filter (e.g. Lüthi et al. 2005). We could approximate the uncertainty of the particle velocity measurement at the level of 10–15%.

We note that the particle velocity is higher in the positive x direction, parallel to the lid direction and lower in the negative x direction, i.e. at the bottom. Vertical velocity is almost symmetrically distributed, and the spanwise velocity component, w, exhibits narrower distribution. This means that the particles move primarily in the x–y planes with a relatively slow drift between the planes. Nevertheless, the three-dimensional motions of the particles is not negligible. In addition, we observe that the PDF are not Gaussian. The best-fit Gaussian distribution curves seem to be adequate in the low velocity range, but not so for the

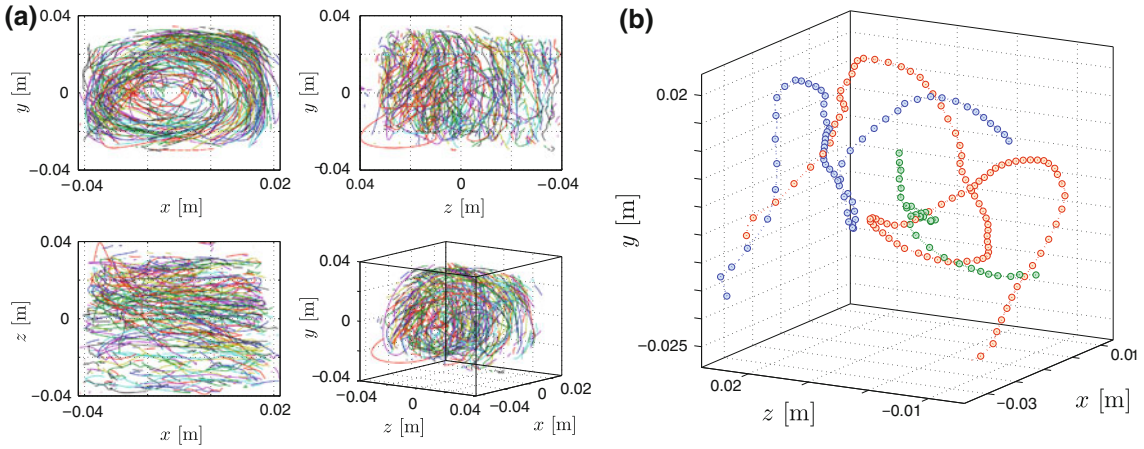

Fig. 6 **a** Three orthogonal views and an isometric view of the Lagrangian trajectories. Geometrical center of the cavity is at −0.01, 0, 0 m, according to the coordinate axis defined in Fig. 1. **b** Samples of Lagrangian trajectories longer than 200 time steps

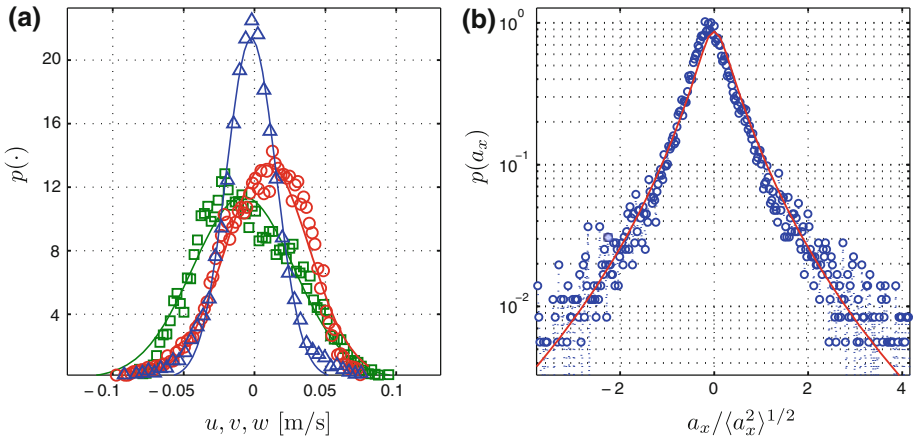

Fig. 7 (**a**) Probability density functions, $p(\cdot)$ of the velocity components, *u*—circles, *v*—squares and *w*—triangles. *Solid lines* are Gaussian best-fit curves. **b** Probability density function of the normalized x-component of acceleration, $p(a_x)$. *Solid line* corresponds to the log-normal fit, $P(x) = \frac{e^{3s^2/2}}{4\sqrt{3}}\left[1 - \mathrm{erf}\left(\frac{ln\left(|x/\sqrt{3}|\right)+2s^2}{\sqrt{2}s}\right)\right]$, best fit for $s \approx 1.42$, ($R^2 = 0.91$) that leads to very high flatness $F = \frac{9}{5}e^{4s^2} \sim 30$

higher values. This deviation of the distributions from the Gaussian can be explained by the specific features of the lid-driven cavity flow. High velocity values appear only in few regions: close to the lid, in the downstream jet and next to the secondary eddies (see, e.g. Kreizer et al. (2010) Fig. 1, 4 and 6), mainly due to the interactions of the fluid and particles with the lid and with the domain boundaries.

Similarly, the Lagrangian acceleration of a particle is calculated through the Lagrangian derivative of the velocity vector in time, $\boldsymbol{a} = DV(t)/D(t)$. Lagrangian acceleration is considered to be one of the key quantities in studies of turbulence or of particle motion in turbulence, (e.g. Xu and Bodenschatz 2008, Toschi and Bodenschatz 2009, among others). Following these works, we present a PDF of the normalized acceleration component $p(a_x)$ in Fig. 7b. The acceleration component is normalized with the respective root mean square, $\langle a_x^2 \rangle^{1/2}$. For the sake of comparison, we added a solid line that emphasizes the log-normal distribution fit: $P(x) = \frac{e^{3s^2/2}}{4\sqrt{3}}\left[1 - \mathrm{erf}\left(\frac{ln\left(|x/\sqrt{3}|\right)+2s^2}{\sqrt{2}s}\right)\right], \quad s \approx 1.42,$ which is typically used for the acceleration distribution models, (e.g. Beck 2007). The flatness of this distribution is high, $F = \frac{9}{5}e^{4s^2} \approx 30$, pointing to the strong deviation from the Gaussian distribution and fat tails. The acceleration distribution is in an agreement with the numerical and experimental studies of Mordant et al. (2004); Volk et al. (2007); Qureshi et al. (2007); Xu and Bodenschatz (2008).

4 Summary and conclusions

This work demonstrates the cost-effective particle tracking system using real-time image processing and the specially designed optical setup of the image splitter and back-side mirrors that provide four views of the observational volume.

The use of FPGA integrated into camera electronics and of real-time image processing algorithm significantly reduces the data transfer rates. Instead of images, binary data that contains the object center-of-mass position, size and total intensity are transferred to the host PC. Reduced data rates enable particle tracking experiments with

remotely controlled cameras, connected by a standard Ethernet network. On the other hand, the strongly reduced data rate allows for significantly longer duration of experiments using a direct writing access to the hard drive or another storage device.

The optical design is performed using a home-made open-source software, freely available for download. The software allows to design a splitter and defines the location of the mirrors, depending on the observation volume size, position of the camera and angles of the four views. The use of a single camera simplifies the tracking method as it eliminates the necessity of high-precision multi-camera synchronization. The drawback lies in the seeding density, which should be lower when compared to the multi-camera 3D-PTV systems, due to a reduced number of pixels per single view.

This experimental setup is less cumbersome than the existing solution of the 3D-PTV system with customized solutions for streaming and storage of high data rates. An open-source software is available for particle tracking and optical design and could help research groups interested in Lagrangian description of the flow to adopt the particle tracking method. In addition, unsupervised remotely operated particle tracking experiments with a long-duration storage capability, useful in harsh environments, large-scale flow facilities, microgravity or underwater applications, become possible.

Acknowledgments The authors wish to thank Matthias Kinzel for providing the drawings and Beat Lüthi for the ETH Zurich optical setup. The authors are thankful to David Ratner and Reut Elfassi from the Turbulence Structure Laboratory for the assistance with the experiments and technical support of the experimental setup and to Eldad Sumner for the design of the optical system. We thank our anonymous reviewers for helpful comments. The research was supported by the Israel Science Foundation under grant no. 782/08 and the Wolfson Family Charitable Trust.

References

Arroyo MP, Greated CA (1991) Stereoscopic particle image velocimetry. Meas Sci Tech 2(12):1181–1186

Bardet P, Peterson P, Savaş O (2010) Split-screen single-camera stereoscopic PIV application to a turbulent confined swirling layer with free surface. Exp Fluids 49(2):513–524

Beck C (2007) Statistics of three-dimensional Lagrangian turbulence. Phys Rev Lett 98(6):064502

Chan KY, Stich D, Voth GA (2007) Real-time image compression for high-speed particle tracking. Rev Sci Inst 78(2):023704

Dracos T (ed) (1996) Three-dimensional velocity and vorticity measuring and image analysis techniques. Kluwer, Dordrecht

Dupont O, Dubois F, Vedernikov A, Legros JC, Willneff J, Lockowandt C (1999) Photogrammetric set-up for the analysis of particle motion in aerosol under microgravity conditions. Meas Sci Tech 10:921–933

Guala M, Liberzon A, Hoyer K, Tsinober A, Kinzelbach W (2008) Experimental study on clustering of large particles in homogeneous turbulent flow. J Turb 9(34):1–20

Hoyer K, Holzner M, Lüthi B, Guala M, Liberzon A, Kinzelbach W (2005) A scanning technique for particle tracking velocimetry. Exp Fluids 39:923–934

Kreizer M, Ratner D, Liberzon A (2010) Real-time image processing for particle tracking velocimetry. Exp Fluids 48(1):105–110

Lobutova E, Resagk C, Rank R, Müller D (2009) Extended three dimensional particle tracking velocimetry for large enclosures. In: Nitsche W, Dobriloff C (ed) Imaging measurement methods for flow analysis. Springer, Berlin, pp. 113–124

Lüthi B, Tsinober A, Kinzelbach W (2005) Lagrangian measurement of vorticity dynamics in turbulent flow. J Fluid Mech 528:87–118

Mordant N, Crawford AM, Bodenschatz E (2004) Three-dimensional structure of the Lagrangian acceleration in turbulent flows. Phys Rev Lett 93(21):214501

Nimmo Smith WAM (2008) A submersible three-dimensional particle tracking velocimetry system for flow visualization in the coastal ocean. Limnol Oceanogr Methods 6:96–104

Nobach H, Bodenschatz E (2009) Limitations of accuracy in PIV due to individual variations of particle image intensities. Exp Fluids 47(1):27–38

Qureshi NM, Bourgoin M, Baudet C, Cartellier A, Gagne Y (2007) Turbulent transport of material particles: an experimental study of finite size effects. Phys Rev Lett 99(18)

Toschi F, Bodenschatz E (2009) Lagrangian properties of particles in turbulence. Ann Rev Fluid Mech 41:375–404

Tsorng S, Lai J, Capart H, Young D (2006) Three-dimensional tracking of the long time trajectories of suspended particles in a lid-driven cavity flow. Exp Fluids 40(2):314–328

Tsorng SJ, Capart H, Lo DC, Lai JS, Young DL (2008) Behaviour of macroscopic rigid spheres in lid-driven cavity flow. Int J Multiphase Flow 34(1):76–101

Volk R, Calzavarini E, Verhille G, Lohse D, Mordant N, Pinton J-F, Toschi F (2007) Acceleration of heavy and light particles in turbulence: comparison between experiments and direct numerical simulations. Physica D 237:2084–2089

Xu H, Bodenschatz E (2008) Motion of inertial particles with size larger than Kolmogorov scale in turbulent flows. Physica D 237:2095–2100